World Wide Journal of Multidisciplinary Education and Research

M. H. Awad
Shendi University, Faculty of Science and Technology, department of Chemistry – Shendi, Sudan.

Khaled A. Hreeba
Faculty of Education Tripoli, University of Tripoli, Suq Aljumea – 40405 – Libya.

Abdulati E.Khalil
Faculty of medical Technology-Surman, Sabratha University – Libya.

Phytochemical Screening, Metal Composition and Biosynthesis of Silver Nanoparticles of *Capparis spinosa* L.(Qapar) leaf from Libya.

M. H. Awad, Khaled A. Hreeba, Abdulati E.Khalil

Abstract

In this study, the dry leaves of C. *spinosa* L. were sequentially extracted using several solvents, such as water, ethanol, chloroform, and ethyl ether. The resulting extracts were subjected to phytochemical screening tests. C. *spinosa* L. leaf extract contains Alkaloids, Carbohydrates, Glycosides, Phytosterols, Saponins, Flavonoids, Tannins, Proteins, and Amino acids. Also, the results obtained showed that the cardiac glycoside and Tannins were present throughout all solvent extracts, while the Quinones were absent in the studied C. *spinosa* L. leaves. The Flame photometry data indicates that the C. *spinosa* L. leaves is rich in minerals such as K, Na, Ca and Ba. Silver nanoparticles (Ag-NPs) have been successfully synthesized using C. *spinosa* L. leaf extract and the nature of the synthesized nanoparticles was analyzed by UV-Vis spectroscopy, FTIR, and XRD. The UV- Visible spectroscopy showed absorption peak at around 470 nm and at high extract concentration the absorption peak shifted to 430 nm. FTIR spectra showed that the biomolecules present in the extract were responsible for the reduction of Ag^+ to Ag^0 and the formation of Ag-NPs. The XRD study confirmed that the main product is Ag-NPs possessing a face-centered cubic structure with an average crystalline size of 16.14 nm.

Introduction

The *C. spinosa* L. bush is a perennial plant that bears rounded, fleshy leaves and large, white to off-white flowers. The genus C. *spinosa* belongs to the *Capparidaceae* family, and grows naturally from the Atlantic coast of Morocco through the Mediterranean to the Black Sea, in Crimea and Armenia, and to the eastern side of the Caspian Sea and Iran [1,2]. The family of this plant species may have originated in the tropics, and later, by natural factors, it spread to the Mediterranean basin [3], and its distribution in southern Europe, Arabia and the Middle East to China has also been reported [2]. Since ancient times, medicinal plants have been used as therapeutic agents for treatment of many diseases because they have health-promoting effects and contain bioactive and antioxidant components such as flavonoids, phytosterols, glucosinolates, polyphenols, carotenoids, coenzyme, and tannins [4]. In Libyan folk medicine, *C. spinosa* leaves are used to treat many diseases, such as hepatotoxicity, nephropathy, cancer and skin diseases. The medicinal effect of C. *spinosa* leaves is due to them being rich in glucosinolates and flavonoids, including rutin and quercetin. Rutin is rutinoside, which is quercetin with the hydroxyl group at the C-3 position replaced by glucose and rhamnose sugar groups. It also has the role of a metabolite and antioxidant. It is derived from the disaccharide, quercetin O-glucoside, tetrahydroxyflavone and rutinoside.

There are many methods for the biosynthesis of Ag-NPs, such as green synthesis methods [5], electrochemical [6], and thermal decomposition [7]. The green synthesis of silver or gold nanoparticles using medicinal plant extract has been studied expansively because of their unique physicochemical characteristics including antimicrobial properties, catalytic activity, electronic properties, magnetic properties, and optical properties. The previous effects are related to their extremely small size and large surface to volume ratio [8]. Recently, a number of researchers biosynthesized Ag-NPs compounds from the aqueous extract of *C. spinosa* leaves, Benakashani et al. reported that from the disc diffusion results, the biosynthesis of Ag-

Correspondence:
M. H. Awad
Shendi University, Faculty of Science and Technology, department of Chemistry – Shendi, Sudan.

NPs from aqueous extract of *C. spinosa* leaves showed an excellent antibacterial property and a high antimicrobial activity compared to the ionic silver [9], the same results were reported by Saleh et al. [10], while Katrin et al. reported that the biosynthesis of Ag-NPs from aqueous extract of *C. spinosa* leaves could be applied as antifungal agents for biological control of food spoiling and also as a new therapeutic agent against fungal infections in human and animals [11]. The aim of this study is to investigate the phytochemical constituents of *C. spinosa* leaf extracts and evaluate the level of essential and heavy elements in *C. spinosa* leaves using flame photometer and atomic absorption techniques. The study also aims to perform a green synthesis Ag-NPs using *C. spinosa* leaves extract as the reducing agent.

Material and methods
Sample collection and preparation

The plant samples for this study were collected from Nafusa Mountains- Kikla city- in the western Tripolitania region – northwestern Libya. The leaves were washed, cleaned, dried at 60 ºC overnight, and the dry leaves were ground to fine powder using a pestle and mortar (Fig.1). 12g of the sample was accurately weighed into four different 500 mL beaker and 300 mL each distilled water, ethanol, chloroform, and ether were added to the beakers respectively. These were left for 72 hours. The crude extracts were then decanted and kept for the various analyses. The extraction yield was calculated as the ratio between the weight of the dry extract obtained after evaporation and the initial weight of the dry leaf sample. The yield is calculated by the following equation:

$$Yield\ (\%) = (W_0/W_1) \times 100$$

where W_0 is the weight in grams of the dry extract and W_1 is the weight in grams of the dry leaf sample.

Fig. 1: Photograph of C. *spinosa* L. (A) plant (B) leaves (C) leaf powder.

Physicochemical and phytochemical screening analysis
Moisture content was determined according to FAO Paper No. 49 (1990) after incubating a sample of fine powder of C. *spinosa* L. leaves at 105 °C for 24 hrs. [12, 13]. The ash content was measured by burning the dry powder sample in a muffle furnace at 550 °C for 6 hrs. [14,15]. The phytochemical screening of C. *spinosa* L. leaf sample was recorded according to the standard methods mentioned by Zaid et al., and Njoku et al. [8,16].

Metal composition
The amount of the essential elements in *C. spinosa* L. leaf sample was calculated according to the standard method mentioned by Salama et al.[17], where 1 g of the dry sample was weighed in a porcelain crucible of known weight, then it was placed inside a muffle furnaces at a temperature of 550 ºC., for five hours, then the ashes were transferred quantitatively by distilled water into a 100 mL volumetric flask contains 5mL of 1M nitric acid, then the solution was warmed until the ash is completely dissolved. Then the solution was cooled and completed to the mark by a Distilled water. The concentration of several elements such Li, Ba, Ca, K, Na was determined using a BWB flame photometer.

Silver Nanoparticle Preparation
100 mL of silver nitrate solution (1mM) was placed on a magnetic stirrer and the temperature was monitored at 20 °C. Then different volumes of the leaf extract were added to the silver nitrate solution, a stop watch was run, and the changing color of the solution was observed over time. The resulting solution was concentrated by centrifugation at

4000 rpm for 45 mints. The supernatant layer was transferred to a beaker for further sedimentation of particles and repeated centrifugation was carried to purify Ag-NPs. The resulting product was dried in the incubator. The obtained molecules were stored for further characterization.

FTIR spectroscopy and UV Measurements
FTIR spectroscopy of extracted leaf and silver nanoparticle samples was measured on a FTIR spectrometer (Spectrum Rα I advanced operation, Perkin Elmer precisely, USA). 0.01 g of sample was mixed with 0.2 g KBr, then the mixture was pressed to form a transparent disc. The IR spectrum of dried samples were characterized in the range 4000 - 400 cm^{-1}. UV-Vis absorption spectra were measured using the Jenway Spectrophotometer-6300 Designed and manufactured in U.K. by Jenway Ltd. Absorption of a spectrophotometer over the range 400 to 900 nm was recorded.

XRD Analysis
The particle size of synthesized Ag-NPs were determined by X-ray diffraction spectroscopy. The synthesized Ag-NPs were studied with CUKα radiation at voltage of 30 kV and current of 20 MA with a scan rate of 0.030/s. Different phases present in the synthesized samples were determined by X′ pert high score software with search and match facility. The Crystalline size (D), micro-strain (ε) [18], dislocation density (δ) [19], and stacking fault (SF) [20] of the synthesized Ag-NPs were calculated using the following equations:

D (nm) = K× λ / ($\beta\ cos\theta$) = (0.9 × 0.15406) / ($\beta\ cos\theta$)

Where D is the crystal size, K is a constant value that depends on the actual shape of the crystallite, λ is the wavelength of an X-ray , β is the full width at half maximum of the peak in radians, and **θ** is the Braggs angle in radians.

$$\varepsilon = \beta \cos\theta / 4$$
$$\delta = 1 / D$$
$$SF = \left[\frac{2\pi^2}{45(3tan\theta)^{0.5}}\right]\beta$$

Results

Table 1 shows that the moisture and ash content of C. *Spinosa* L. leaf were found to be ranged from 8.39 to 11.57 % with mean value 9.57% . while the ash content were found to be ranged from 18.72 to 22.38% with mean value 21.18%. Table 1 shows that the *C. spinosa* L. leaf sample is rich in sodium, calcium, and potassium. An appreciated amount of barium was also detected, while lithium was not detected in the leaf sample. The mineral compositions were calculated based on dry leaf sample and the major elements were in the order Na > Ca > K for C. *spinosa* L. leaf. Calcium is the main component of the skeleton. In addition, calcium has some physiological activities such as blood coagulation and convulsion and excitation of muscles. Potassium ions play an important role in the maintenance of the cardiac rhythm and in constipation[8,14].

Table 1: physicochemical data (X ± SD) of *C. Spinosa* L. leaf.

Sample	Moisture (w/w%)	Ash (w/w%)	Metal composition (g/kg)				
			Na	Ca	K	Ba	Li
C. Spinosa **L. leaf**	9.57 ±1.3	21.18± 1.5	14.59±0.66	6.02±0.25	3.27±0.66	1.28±0.06	ND

Table 2 shows that the extractive yield of C. *spinosa* L. leaves were found to be 6.11, 4.70, 1.28 and 0.75% for water, ethanol, chloroform, and diethyl ether, respectively. This order shows that the leaves of the C. *spinosa* L. plant are rich in highly polar compounds, such as phenolic compounds, due to their richness in hydroxyl groups [21,22]. Therefore, the difference in extraction yields obtained using different solvents depends on the chemical properties of the molecules to be extracted, the physicochemical properties of the solvents used, and in particular their polarity, which affects the solubility of the chemical components of the sample [23].

Table 2: Extractive values (X ± SD) and phytochemical screening of solvents extract of *C. Spinosa* L. leaf.

Solvents		Water	Ethanol	Chloroform	Ethyl ether
Phytochemical constituents	**Extractive values (w/w %)**	6.11 ±1.5%	4.70 ±1.4	1.28±0.6	0.75± 0.4
Alkaloids	Mayer's	++	-	++	-
	Wagner's	++	-	-	-
	Dragendorff 's	+++	-	+	+
	Hager's	+++	-	+	+
Carbohydrates	Molisch's	+++	+++	+	+
	Benedict's	-	-	-	-
	Fehling's	++	+++	+	-
Glycosides	Borntrager's	-	-	-	-
	Legal's	-	-	-	-
	Keller-Killiani	+	++	+++	++
Saponins		++	-	+	-
Flavonoids	Lead acetate	-	+	+++	++
Tannins	FeCl₃ test	+++	++	++	+
Phytosterols	Salkowski's	-	+	+++	-
Proteins and Amino acids	Xanthoproteic	+	+	++	-
	Ninhydrin	+++	-	++	+
Quinones		-	-	-	-
Terpenoids		++	++	++	+

Legend: (+++ = Abundance); (++ = Moderate); (+ = Trace); (- = Absent).

The phytochemical screening of *C. spinosa* L. leaves revealed the presence of alkaloids in high quantities in water extract, but alkaloids were absent in ethanol extract. Helmut Wiedenfeld mentioned that alkaloids such as Pyrrolizidine alkaloids are toxic to humans [24], but the *C. spinosa* L. leaves consist of non-toxic alkaloids such as stachydrine and 3-hydroxystachydrine [25]. Also, Essiett and Ukpong reported that the presence of alkaloid compounds in plant tissues acts as a nutrient and toxin repellent for herbivores because they interact directly with special molecules at target sites within the nervous system [26]. The presence of glycosides in all extracts was investigated by the Keller-Killiani test for C. *spinosa* leaves, consistent with the reports of Hongxia et al., [27]. The Keller-Killiani test showed that C. *spinosa* leaves contain glycosides. Saponins were also present in distilled water and chloroform extracts. Saponins were abundantly present in aqueous extract compared with chloroform extract. Sofowora revealed that saponins exhibit a wide range of biological activities, such as anti-inflammatory, anti-fungal, anti-parasitic, anti-tumor activities, and anti- viral [28]. Flavonoids were present in abundance in the chloroform extract, with a moderate value in the ethyl ether extract, and appeared at a trace value in the ethanol extract, while it was absent in the aqueous extract. *C. spinosa* L. leaves are rich in hydroxylated phenolic compounds such as Quercertin and Rutin have received great attention for their positive impact on health due to their antioxidant effect [29]. Both rutin and quercetin are non-toxic flavonoids. Rutin is safe up to 2000 mg / kg, while quercetin is non-toxic up to 5000 mg/kg [30,31]. The study also revealed the presence of tannins in all extracts. It was observed that tannins were in abundance in aqueous extract, with a moderate value in the ethanol and chloroform extracts, and appeared at a trace value in the ethyl ether

extract. The presence of tannin compounds in the leaves of C. *spinosa* L. could be beneficial in the antifungal activity of these leaves [32]. Quinones were absent in all extracts, while terpenes were found in all extracts in moderate quantities except for ethyl ether extract, which appeared as a trace.

The presence of these bioactive compounds in the leaves of *C. spinosa* L. indicates their potential for use in the green synthesis of Ag-NPs complexes. Fig. 2 shows that when different volumes of aqueous extract of C. *spinosa* leaves are added to 100 mL of (1mM) silver nitrate it shows a color change from pale brown to dark brown, indicating the formation of Ag-NPs. The appearance of the color is due to the excitation of surface plasmon resonance (SPR) by Ag-NPs. Silver nanoparticles have free electrons that play an important role in the appearance of color, which gives rise to the SPR absorption band, due to the combined vibration of electrons of Ag-NPs in resonance with the light wave. The bioreduction reaction of leaf extract of C. *spinosa* with silver

nitrate was confirmed by the UV–visible spectra. Absorption spectra of Ag-NPs appeared at 470 nm after one week of incubation at 20 $^{\circ}$C., while silver nitrate solution and aqueous extract of C. *spinosa* leaf alone did not show any absorption peak between wavelengths 400 to 800 nm. Fig.2 shows that the peak intensity increased with increase of aqueous extract concentration from 5.0 mL to 10.0 mL, and above that, the peak intensity decreased at 15.0 mL and disappeared at concentration up to 20.0 mL until 50.0 mL, but at high concentration 80 mL blue shift occurred and peak with low intensity and narrow width was appeared at 430 nm as shown in Fig.2, which is the characteristic absorption of spherical Ag-NPs, this band corresponds to the absorption by colloidal Ag-NPs in the region (400 to 450 nm) due to the excitation of surface plasmon vibration. A high concentration of C. *spinosa* L. leaf extract increases the number of bio-compounds required to reduce Ag^+ to Ag^0.
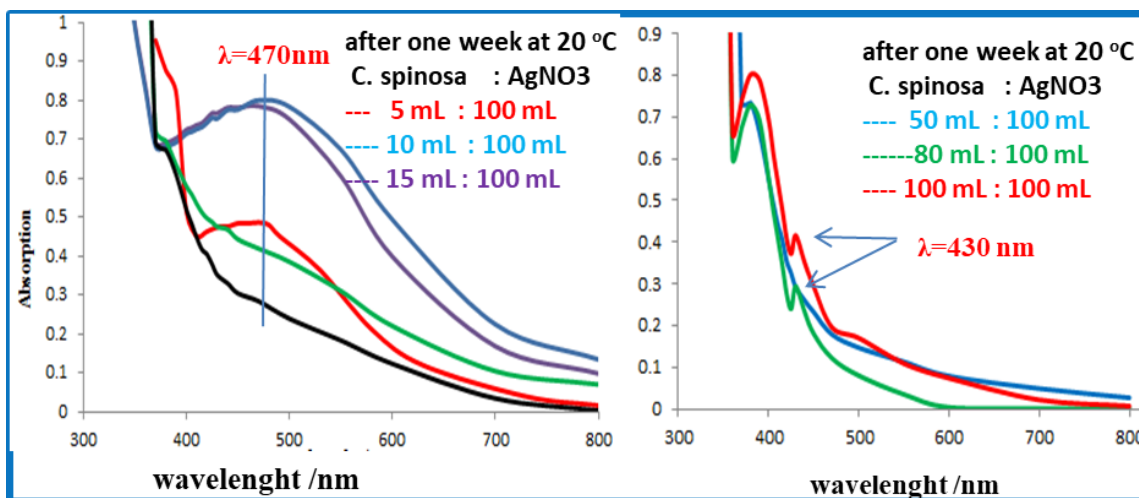

Fig. 2: UV–Vis spectra of synthesized Ag-NPs at different concentrations.

Fig. 3 shows that the band intensity of solution (10:100 mL) was increased with increasing bioreduction reaction time up to seven days, and after the eighth day the band intensity decreased. The increase in the band intensity of the Ag-NPs absorption is due to the concentration of silver particles

increasing with reaction time. When the reduction time continued, after eight days, the absorption band did not change and appeared at 470 nm, indicating that the Ag-NPs formed had the same particle size and shape.
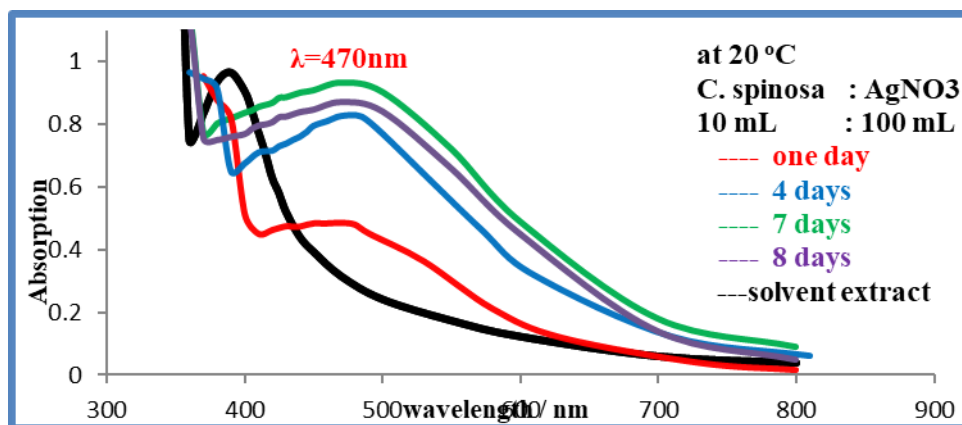

Fig. 3: UV–Vis spectra of synthesized Ag-NPs formation with time.

Fig.4 shows that the FTIR spectra of the C. *spinosa* L. leaf extract suggested the presence of O-H and N-H (amide) at 3256 cm^{-1}, C-N bond in amide present at 2358 and 2338 cm^{-1}, carbonyl groups at 1592 and 1652 cm^{-1}. A strong peak at 1594 cm^{-1} is assigned for the NH$_2$ absorption band [33], and

for C=C stretching vibration bond in the aromatic ring confirming the presence of the aromatic group, while a weak peak at 1652 cm^{-1} is probably for C=C normal alkene. All weak peaks ranging from 1699 to 1843 cm^{-1} are probably for carbonyl groups C=O, after the synthesis of Ag-NPs the

FTIR spectra showed that all the peaks were slightly shifted to a higher wave number. Fig.4 shows that the FTIR spectrum of Ag-NPs consists of six fundamental bands. The broad band at 3284 cm^{-1} is most likely for N-H bond and groups O-H stretching vibration and H-bond of phenols and alcohols. The weak peak at 2948 cm^{-1} is probably for aliphatic C-H symmetry stretching vibration, while the two weak beaks at 2335 and 2359 cm^{-1} are probably for C-N asymmetric stretching vibration. The broad band at 1601 cm^{-1} is probably C=C bond in aromatic ring. The broad band occurring at 1381 cm^{-1} is probably for -CH$_3$ bend vibration, and the strong band at 1074 cm^{-1} was assigned to C–C and C-O bonds. The weak peaks at 892 to 728 cm^{-1} were characterization of out of the plane deformation vibration of C-H bond in aromatic components [34]. In the FTIR spectra of the extract, the peaks of C=O carbonyl groups that ranged from 1699 to 1843 cm-1 were disappeared in the FTIR spectra of formed Ag-NPs, which might be responsible for the bioreduction reaction and formation of Ag-NPs.
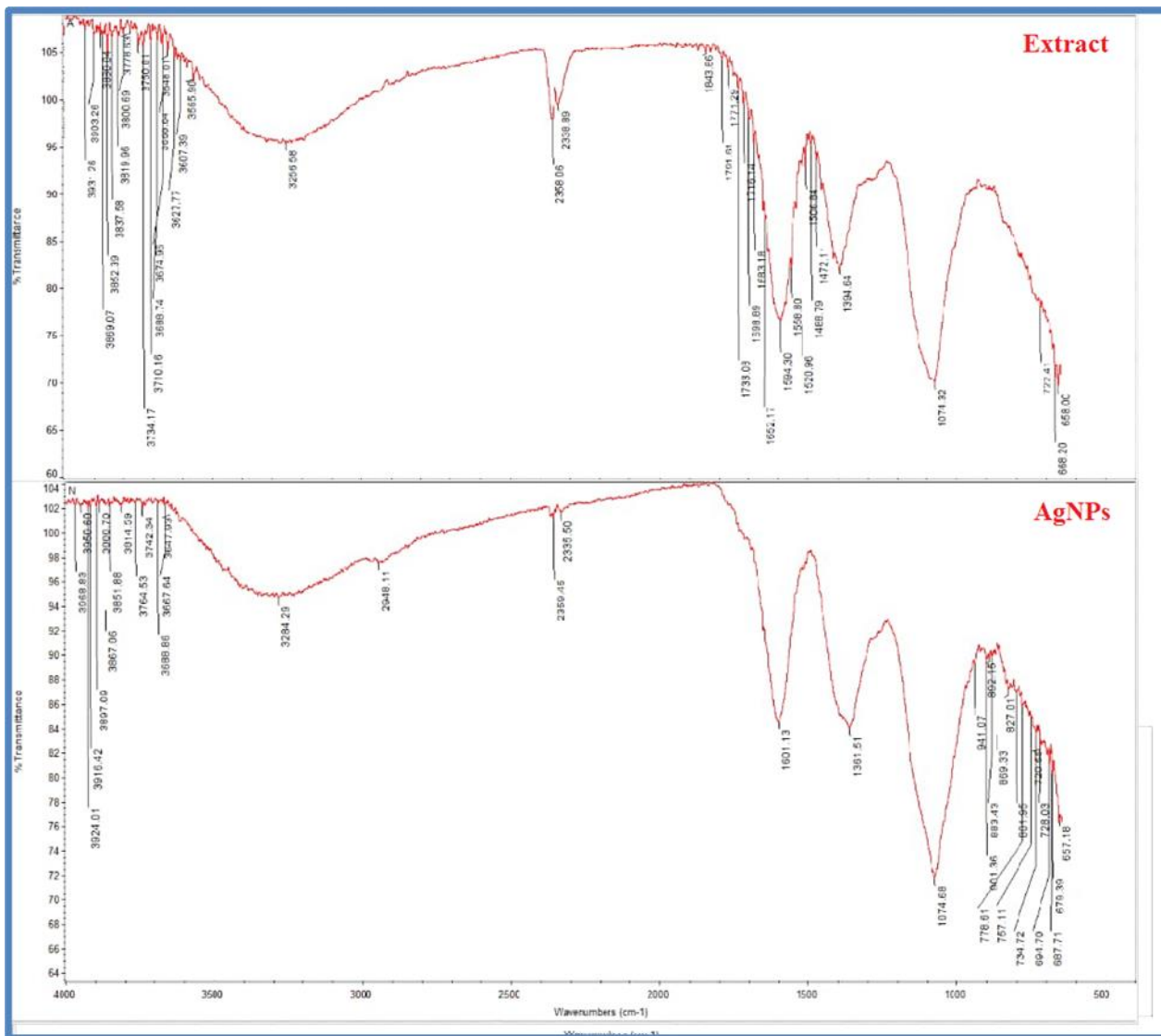

Fig. 4: FTIR spectra of Ag-NPs prepared by mixing 10 mL of extract with 100 mL of (1 mM) silver nitrate.

Silver nanoparticles prepared by Turkevich chemical method were characterized using powder XRD to confirm the molecular size of the silver product and find out the compositional information. Table 6 shows the structural parameters of Ag-NPs, obtained from a ratio (10:100 mL) of extract concentration to (1mM) silver nitrate solution, and Fig. 5 shows the XRD pattern of Ag-NPs.

Table 3: Structural parameters of Ag-NPs, obtained from ratio (10:100 mL) of extract concentration to (1mM) silver nitrate solution.

Pos. [°2Th.]	FWHM Left [°2Th.]	Crystalline size D (nm)	Inter- planar spacing d (A^0)	Lattice constant a (Å)	Specific Surface Area (m^2/g)	Micro strain ε x 10^{-3}	Dislocation Density δ x 10^{15} (m^{-2})	Stacking Fault x 10^{-3}
38.817	0.551	15.289	4.637	8.032	37.375	2.268	4.27995	1.307
44.694	0.472	18.185	4.055	8.110	31.423	1.906	3.02377	1.037
64.024	0.629	14.877	2.907	8.222	38.410	2.330	4.51820	1.121
77.823	0.630	16.212	2.454	8.139	35.247	2.138	3.80476	0.986

Table 3 and Fig. 5 showed that the main peaks in the XRD pattern of the bioreduction reaction of 10 mL of leaf extract with 100 mL of silver nitrate indicated that the main product of the reaction is the Ag-NPs. Fig.5 shows the XRD spectrum of Ag-NPs which consists of diffraction peaks around 38.82°, 44.74° , 64.02° , and 77.82°, which were identified as due to silver metal and corresponding to (hkl) values (111), (200), (220), and (311) of the cubic face-centered silver (fcc). The XRD pattern showed that the main composition of the nanoparticle was silver. There are seven more weak peaks, at 15.21°, 26.14°, 28.29°, 32.35°, 46.69°, 49.74°, and 72.98°. These peaks were related to the formation of traces of Ag_2O nanoparticles because the same peaks were recorded by Zuzer et al., when studying the synthesis of silver oxide nanoparticles using good bacteria (*Lactobacillus mindensis*)[35]. The mechanism of the oxidation reaction that produces traces of silver oxide from an unknown oxidizing agent during the bioreduction reaction of Ag^+ to Ag^0 has not been reported, so further studies are needed in this direction to determine the exact mechanism used in the manufacture of pure Ag-NPs. According to the Debyee Scherrer equation, the crystalline size was found to range from 14.877 to 18.185 nm with an average of 16.140 nm. The same result was reported by Benakashani et al. with the crystalline particle size equal to 20 nm [9]. The value of the interplanar spacing (d) between the atoms for a simple cubic (a = b = c = a_0) has been calculated using Braggs Law, $2d \sin \theta = n\lambda$, where n is the order of diffraction pattern and it was equal to 1, (Most accurate d-spacing's are those calculated from high-angle peaks). Table 3 shows that the interplanar spacing (d) of the four peaks equal 4.687, 4.055, 2.907, and 2.454 A^0.

The Lattice constant values (a) have been calculated from the (d) values using the formula, $a = d \times \sqrt{(h^2 + k^2 + I^2)}$, where the $(h^2 + k^2 + I^2)$ values equal $(1^2 + 1^2 + 1^2)$, $(2^2 + 0^2 + 0^2)$, $(2^2 + 2^2 + 0^2)$, and $(3^2 + 1^2 + 1^2)$ for the diffraction peaks (111),(200),(220), and (311) respectively. Table 3 shows that the four values of the Lattice constant (a) ranged from 8.032 to 8.222 Å with the mean value 8.126 Å, and it is seen that the four values are nearly the same. The specific surface area (S) was also calculated from the particle size value (D) using the Brumauer Emmete Teller (BET) equation: $S = 6 \times 10^3/D \times \rho$, where ρ is the density of silver 10.5 g/cm^3, and D is the crystalline size of the particles because there is no estimated difference between the crystalline size calculated from XRD (nm) using the Debyee Scherrer equation and the particle size calculated from Williamson-Hall (nm), Table 4 shows that the four values of specific surface area (S) ranged From 31,423 to 38,410 m^2/g, with an average value of 35,612 m^2/g.
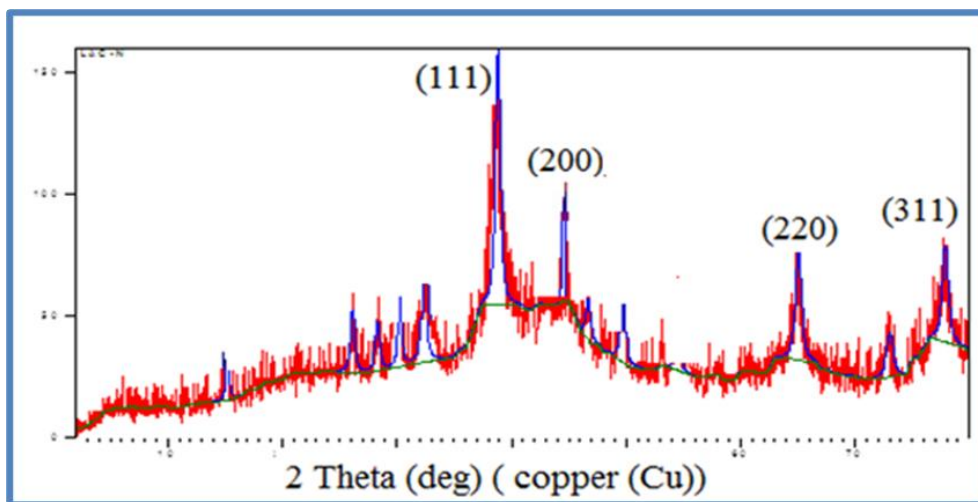

Fig. 5: XRD result for 10:100 ratio Ag-NPs Conclusion.

The study showed that C. *spinosa* L. leaf extract contains alkaloids, carbohydrates, glycosides, phytosterols, saponins, flavonoids, tannins, proteins, and amino acids. Therefore, the C. *spinosa* L. leaves could be a good source for pharmaceuticals. The eco-friendly Ag-NPs were synthesized using the medicinal herb C. *spinosa* L. leaf extract, which provides simplicity, efficiency and was suitable for large scale preparation of Ag-NPs. The color change during the synthesis processes and the presence of a clear peak at 470 nm using a volume of less than 15 mL to 100 mL of silver nitrate confirms the formation of Ag-NPs. FTIR measurements were performed and confirmed the presence of multiple functional groups that have a stronger ability to reduce silver ions and form Ag-NPs. The crystalline size of silver nanoparticles was estimated by the XRD technique and it was found to range from 14.877 to 18.185 nm. Different parameters like Inter- planar spacing, specific surface area, Micro strain , Dislocation Density, and Stacking Fault were studied using XRD. The XRD study confirms that the particles obtained are silver nanoparticles (FCC).

Reference
1. M. H. Shahrajabian, W,I. Sun, Q. Cheng, Plant of the Millennium, Caper (*Capparis spinosa* L.), chemical composition and medicinal uses, Bull Natl Res Cent. 45(131)(2021) 1-9.
2. C. Inocencio, F. Alcaraz, F. Calderon, C. Obon, D. Rivera, The use of floral characters in *Capparis* sect. *Capparis'* to determine the botanical and geographical origin of capers. Eur. Food Res. Technol. 214 (2002) 335-339.

3. M, Zohary, The species of *Capparis* in the Mediterranean and the Near Eastern countries, Bull. Res. Counc. Isr. 8D (1960) 49-64.

4. P. Ansari, F. S. Jannatul , T. K. Joyeeta ,R.R. Musfiqur, M. S. Rahman, B. R Akib , N. A Yasser. S. Veronique, Protective Effects of Medicinal Plant-Based Foods against Diabetes: A Review on Pharmacology, Phytochemistry, and Molecular Mechanisms, Nutrients. 15(3266)(2023) 1-41.

5. N.A. Begum, S. Mondal, S. Basu, R.A. Laskar, D. Mandal, Biogenic synthesis of Au and Ag nanoparticles using aqueous solutions of Black Tea leaf extracts, Colloids Surfaces B Biointerfaces, 71 (1) (2009) 113-118.

6. S. Navaladian, B. Viswanathan, R. Viswanath, T. Varadarajan, Thermal decomposition as route for silver nanoparticles, Nanoscale Res. Lett. 2 (1) (2007) 44-48.

7. M. Starowicz, B. Stypuła, J. Banas, Electrochemical synthesis of silver nanoparticles, Electrochem.Commun. 8 (2) (2006) 227-230.

8. Z. Najah, M. Awad, M. Alshawish, Phytochemical screening, analytical profile and green synthesis of silver nanoparticles of *Senna Alexandrina* Mill, ejbps. 6(12)(2019) 47-53.

9. F. Benakashani , A.R. Allafchian , S.A.H. Jalali , Biosynthesis of silver nanoparticles using *Capparis spinosa* L. leaf extract and their antibacterial activity, Karbala International Journal of Modern Sci. (2016) 1-8.

10. H. S. Saleh, D. Eman, A.A Tahani, A.A. Sulaiman, Green Synthesis, Characterization and Antibacterial Activity of Silver Nanoparticles from *Capparis Spinosa* Leaf Extract , Rev. Chim., 72(1)(2021)145-152

11. E. Katrin, M. Mahboobeh, A. Behnam, S. Sima, S. Asghar, Antifungal Properties of Silver Nanoparticles Synthesized From Capparis Spinosa Fruit, Res Mol Med. 7(4)(2019) 43-50.

12. FAO, Food and nutrition paper, No.49, Rome, 1990.

13. [D. Yebeyen, M. Lemenih, S. Feleke, Characteristics and quality of gum Arabic from naturally grown *Acacia senegal* (Linne) Willd. trees in the central rift valley of Ethiopia, Food Hydrocoll. 23 (2009) 175-180.

14. P.S. Prajna, P.R.. Bhat, Phytochemical and Mineral Analysis of Root of *Loeseneriella arnottiana* Wight, Int. J. Curr. Res. Biosci. Plant Biol. 2(3)(2015) 67-72.

15. M.H. Awad, Aborawi M. Elgornazi, Nouri M.A. Soleiman. Assessment of Physicochemical Properties and Mineral Compositions of Almond (*Prunus amygdalus*) Gum of Libyan Origin, J. Adv. Chem. Sci. 7(1)(2021) 702-705.

16. [O. V. Njoku, Chidi Obi, Phytochemical constituents of some selected medicinal plants, African Journal of Pure and Applied Chem. 3(11)(2009) 228-233.

17. A.S. Salama, A.M. Etorki, M.H. Awad, Determination of Physicochemical Properties and Toxic Heavy Metals Levels in Honey Samples from West of Libya, J. Adv. Chem. Sci. 5 (1)(2019) 618-620.

18. J. P. Richard, I. K. Punithavathy, S. J. Jeyakumar, M. Jothibas, P. Praveen, Effect of morphology in the photocatalytic degradation of methylviolet dye using ZnO nanorods, J. Mater Sci. Mater Electron. 28 (2016) 4025-4034.

19. Y.P. V. Subbaiah, P. Prathap, K.T. Ramakrishna, Structural, electrical and optical properties of ZnS films deposited by close-spaced evaporation, Appl. Surf. Sci. 253 (2006) 2409-2415.

20. B.K. Jena, B.K. Mishra, S. Bohidar, Synthesis of branched Ag nanoflowers based on a bioinspired technique: their surface enhanced Raman scattering and antibacterial activity, J. Phys. Chem. 113 (2009) 14753-14758.

21. T. Gull, F. Anwar, B. Sultana, M.A.C. Alcayde, W. Nouman, *Capparis* species: A potential source of bioactive and high-value components: A review. Ind. Crop. Prod. 67(2015)81-96.

22. I. Rajhi, F. Hernandez-Ramos, M. Abderrabba, M. T. Ben Dhia , S. Ayadi, J. Labidi, Antioxidant, Antifungal and Phytochemical Investigations of *Capparis spinosa* L. Agriculture. 11(2021)1-16.

23. T. Michel, E. Destandau, G. Le Floch, M.E. Lucchesi, C. Elfakir, Antimicrobial, antioxidant and phytochemical investigations of sea buckthorn (Hippophaë rhamnoides L.) leaf, stem, root and seed. Food Chem. 131(2012) 754-760.

24. H. Wiedenfeld, Plants containing Pyrrolizidine Alkaloids - Toxicity and Problems, Food Additives and Contaminants. 28 (03)(2011) 282-292.

25. M. Khatiba, G. Pieraccinib, M. Innocentia, F. Melania, N. Mulinaccia, An insight on the alkaloid content of *Capparis spinosa* L. root by HPLC-DAD-MS, MS/MS and H^1 NMR, Journal of Pharmaceutical and Biomedical Analysis. 123 (2016) 53-62.

26. U. A. Essiett, U. J. Ukpong, Comparative Phytochemical, Nutrient and Anti-Nutrient of Stems of Ipomoea Involucrata Beauv, Ipomoea. Triloba L. and Ipomoea Batatas Lam, American Journal of Food and Nutrition, 2(4)(2014,) 71-76.

27. Z. Hongxia, Z. F. Ma, Phytochemical and Pharmacological Properties of Capparis spinosa as a Medicinal Plant, Nutrients.10 (116)(2018) 1-14.

28. A. Sofowora, A medicinal plants and traditional medicine in West Africa, 3rd edn. John Wiley and Sons Ltd. New York. (2008). 200-203.

29. D. Dekanski, S. Ristic, N.V. Radonjic, N.D. Petronijevic,A. Dekanski, D.M. Mitrovic, Olive leaf extract modulates cold restraint stress-induced oxidative changes in rat liver. J. Serb. Chem. Soc. 76(2011) 1207-1218.

30. R.. Tiwari, M. H. Siddiqui, T. Mahmood, A. Farooqui, P. Bagga, F. Ahsan, A. Shamim, An exploratory analysis on the toxicity and safety profile of Polyherbal combination of curcumin, quercetin and rutin, Clinical Phytoscience. 6(82) (2020) 2-18.

31. S. Patil, H. Somashekarappa, K. Rajashekhar, Evaluation of the radioprotective action of rutin in mice exposed to gamma-radiation. Int J Biol Pharm Res. 3(2012)12-8.

32. M. N.Bouquet, V. L. Harvey, A. H. Debrag, Mechanism of pain in non-malignant disease, curopin support pallat care. 2 (2)(2008)133-228.

33. Z. Zhon, R. Chen, R. Xing, X. Chen, S. Liu, Z. Guo, X. Ji, L. Wang, P. Li, Synthesis and antifungal properties of sulfanilamide derivatives of chitosan, Carbohydr Res. 342(2007) 2390-2395.

34. A. Yadav, A. Kaushik, A. Joshi, Green synthesis of silver nanoparticles using *Ocimum sanctum* L. and *Ocimum americanum* L. for their antibacterial potential, International journal of life science and pharma research. 8(2018) 42-49.

35. H. D. Zuzer, C. Hemlatta, Lactobacillus Mediated Synthesis of Silver Oxide Nanoparticles, Nanomater. nanotechnol. 2 (2012) 1-7.